

# Beam stability analysis of high power laser system based on relay imaging

Jia Xu (徐嘉)<sup>1,2\*</sup>, Jianqiang Zhu (朱健强)<sup>1</sup>, and Fang Liu (刘芳)<sup>1,2</sup>

<sup>1</sup>Shanghai Institute of Optics and Fine Mechanics, Chinese Academy of Sciences, Shanghai 201800, China

<sup>2</sup>Graduate University of Chinese Academy of Sciences, Beijing 100049, China

\*Corresponding author: xujia008@gmail.com

Received December 29, 2011; accepted March 14, 2012; posted online May 16, 2012

The model of a beam propagating in a high power laser system is built based on relay imaging. The displacement sensitivity of the lens to beam positioning error is obtained using this model, which is then compared with the traditional method. Two real systems, the pre-amplifier and four-pass amplifier in SGII-U, are presented to further discuss the differences between the two methods. The limitation and application range are summarized in the end. The findings can be used to provide guidance in similar systems.

OCIS codes: 140.3280, 140.3425, 220.1140, 080.3620.

doi: 10.3788/COL201210.091401.

The high power laser system for inertial confinement fusion (ICF) is a precise, large facility with numerous components, the most important of which are the confocal lens pairs in the spatial filters (SFs). Relay imaging achieved with the confocal lens pairs is a distinctive and significant property in high power laser systems. In Refs. [1,2], relay imaging in the nearfield permits near-uniform filling of amplifier apertures, while keeping whole beam self-focusing and diffraction effects in check. In Ref. [3], the references used for beam auto-alignment are provided through relay imaging in the nearfield and the farfield.

As a beam traverses the numerous components of a high power laser system, inherent but undesirable deviations caused by structural excitation, thermal excitation, and so on, can develop and increase inevitably. The deviations are represented by beam positioning errors in the farfield<sup>[3]</sup> and increase with relay imaging. Relay imaging in the farfield can also be used to analyze beam stability in a high power laser system, but no theoretical analysis has yet to be reported. This letter builds the beam propagation model of several sequential lens pairs, and provides an analysis method of beam stability in a high power laser system based on relay imaging.

A relay imaging system consists of several imaging units  $IU_s$ . The in-out model of the  $k$ th IU ( $IU_k$ ) is depicted in Fig. 1. A beam passes through the previous components and focuses on a spot in the farfield, where

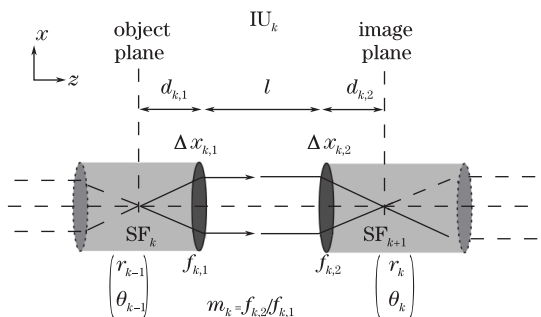


Fig. 1.  $k$ th IU ( $IU_k$ ) in high power laser systems.

it inputs to  $IU_k$  with  $(r_{k-1}, \theta_{k-1})'$ . Then, it traverses two lenses that drifts from their designed positions with  $\Delta x_{k,1}$  and  $\Delta x_{k,2}$  respectively, and outputs with  $(r_k, \theta_k)'$  on the image plane where the spot is relayed. To take structural drifts into account, an augmented matrix in Eq. (2) is used to build the beam propagation model of misaligned optical system<sup>[4,5]</sup>. According to Ref. [5], the relationship between  $(r_{k-1}, \theta_{k-1})'$  and  $(r_k, \theta_k)'$  is given by

$$\begin{pmatrix} r_k \\ \theta_k \\ 1 \\ 1 \end{pmatrix} = t_k \begin{pmatrix} r_{k-1} \\ \theta_{k-1} \\ 1 \\ 1 \end{pmatrix}, \quad (1)$$

$$t_k = \begin{pmatrix} -m_k & B_k & E_k & 0 \\ C_k & -\frac{1}{m_k} & F_k & 0 \\ 0 & 0 & 1 & 0 \\ 0 & 0 & 0 & 1 \end{pmatrix}, \quad (2)$$

$$m_k = f_{k,2}/f_{k,1}, \quad (3)$$

$$B_k = -m_k d_{k,1} - \frac{d_{k,2}}{m_k} + f_{k,1} + f_{k,2}, \quad (4)$$

$$E_k = \Delta x_{k,2} + m_k \Delta x_{k,1}, \quad (5)$$

where  $t_k$  is the optical transfer matrix,  $m_k$  is the magnification index, and  $r_k$  and  $\theta_k$  are the output positioning and pointing error, respectively. The relationship of in-out positioning errors  $IU_k$  is given by

$$r_k = (-m_k r_{k-1} + B_k \theta_{k-1}) + (\Delta x_{k,2} + m_k \Delta x_{k,1}). \quad (6)$$

In terms of geometrical optics, the object in the plane  $d_{k,1}$  is imaged on the plane  $d_{k,2}$  with magnification index  $m_k$  if

$$B_k = -m_k d_{k,1} - \frac{d_{k,2}}{m_k} + f_{k,1} + f_{k,2} = 0. \quad (7)$$

Given that Eq. (7) is satisfied for all  $k$ , the object is repeatedly reimaged or relayed throughout the optical train. When

$$\begin{cases} d_{k,1} = f_{k,1} \\ d_{k,2} = f_{k,2} \end{cases} \Rightarrow B_k = 0, \quad (8)$$

Eq. (6) becomes

$$r_k = -m_k r_{k-1} + (\Delta x_{k,2} + m_k \Delta x_{k,1}). \quad (9)$$

It shows explicitly how the magnification of the IU,  $m_k$ , amplifies the positioning error of input beam  $r_{k-1}$  to the output beam  $r_k$ .

When Eq. (7) is satisfied for all  $k$ , the optical system can be regarded as a combination of sequential IU $_k$ , where  $k=1, 2, \dots, N$ . The positioning error on the  $N$ th image plane can be obtained by iterating Eq. (9), shown as

$$r_N = q_0 r_0 + \sum_{k=1}^N (q_{k,1} \Delta x_{k,1} + q_{k,2} \Delta x_{k,2}), \quad (10)$$

$$\begin{cases} q_0 = (-1)^N \prod_{k=1}^N m_k = (-1)^N \frac{f_{1,2}}{f_{1,1}} \dots \frac{f_{k,2}}{f_{k,1}} \dots \frac{f_{N,2}}{f_{N,1}} \\ q_{k,1} = \prod_{j=k}^N m_j = \frac{f_{k,2}}{f_{k,1}} \cdot \frac{f_{k+1,2}}{f_{k+1,1}} \dots \frac{f_{N,2}}{f_{N,1}} \\ q_{k,2} = \prod_{j=k+1}^N m_j = \frac{f_{k+1,2}}{f_{k+1,1}} \dots \frac{f_{N,2}}{f_{N,1}} \end{cases}, \quad (11)$$

where  $q_0$  is the scale factor of system for input beam positioning error  $r_0$ , and  $q_{k,1}$  and  $q_{k,2}$  are the sensitivities of displacement for the first and second lens in the IU $_k$ , respectively.

For the purpose of comparison, the empirical formula of sensitivity analysis is described in Eq. (12). This is typically used to analyze the beam stability of the ICF system<sup>[6,7]</sup>. The relationship between the positioning error on target ( $r_{\text{Tar},i}$ ) and the movement of lens ( $\Delta x_i$ ) is given by

$$r_{\text{Tar},i} = n \cdot \Delta x_i (f_{\text{Tar}}/f_i), \quad (12)$$

where  $n$  is the number of times that the beam passes through the optical components, and  $f_{\text{Tar}}$  and  $f_i$  are the focal lengths of target lens  $L_{\text{Tar}}$  and the  $i$ th lens  $L_i$ , respectively. The displacement sensitivity of  $L_i$  is given by

$$w_i = n \frac{f_{\text{Tar}}}{f_i}. \quad (13)$$

Given that the final lens along the beam path is the target lens  $L_{\text{Tar}}$  (i.e.  $f_{N,2} = f_{\text{Tar}}$ ), Eq. (11) can be revised as

$$\begin{cases} q_{k,1} = \frac{f_{\text{Tar}}}{f_{k,1}} \left( \prod_{j=k}^{N-1} \frac{f_{j,2}}{f_{j+1,1}} \right) \\ q_{k,2} = \frac{f_{\text{Tar}}}{f_{k,2}} \left( \prod_{j=k}^{N-1} \frac{f_{j,2}}{f_{j+1,1}} \right) \end{cases}. \quad (14)$$

The difference between Eqs. (13) and (14) in a single pass system (where  $n=1$ ) is simply due to the sequential products in brackets in Eq. (14). From Eqs. (13) and (14), we get

$$q_{k,l} = w_{k,l} \prod_{j=k}^{N-1} \frac{f_{j,2}}{f_{j+1,1}}, \quad (n=1, l=\{1,2\}), \quad (15)$$

where the subscript of  $i$  in Eq. (13) is replaced by  $k, l$  to develop a uniform format.

The focal length ratio, i.e., the magnification of SF $_{k+1}$  (shown in Fig. 1), is given by

$$M_{k+1} = \frac{f_{k+1,1}}{f_{k,2}}, \quad (16)$$

then Eq. (15) becomes

$$q_{k,l} = w_{k,l} \prod_{j=k}^{N-1} \frac{1}{M_{k+1}}. \quad (17)$$

It indicates that Eqs. (11) and (13) are congruent in a sequential 4 $f$ -type SF system, in which the magnifications are equal to 1. However, the focal length of lenses in the SFs are usually not equal but designed to be different for the purpose of controlling the location of an image in the high power laser system.

To further illustrate the differences between Eqs. (11) and (13), the pre-amplifier (Fig. 2) and the four-pass amplifier (Fig. 3) in the high power laser system are discussed. The pre-amplifier consists of four SFs, namely, SF $_1$  to SF $_4$  (Fig. 2).

The parameters of the lenses in the pre-amplifier system are listed in Table 1. Based on Eqs. (11) and (13), their sensitivities resulting from both methods are also provided in Table 1 and further illustrated in Fig. 4.

Figure 4 indicates the different results of sensitivity analysis from the relay imaging method and the traditional one. The following information can be gathered:

- there are large differences in sensitivity values between the two methods;
- the sensitivities calculated by the traditional method are much higher;
- and the relative values of the sensitivities of the lenses might be totally opposite, such as  $L_3$  and  $L_8$ , which may lead us to ignore the real sensitive lens during stability analysis and design.

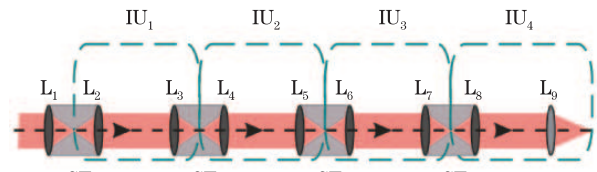


Fig. 2. Structure of the pre-amplifier.

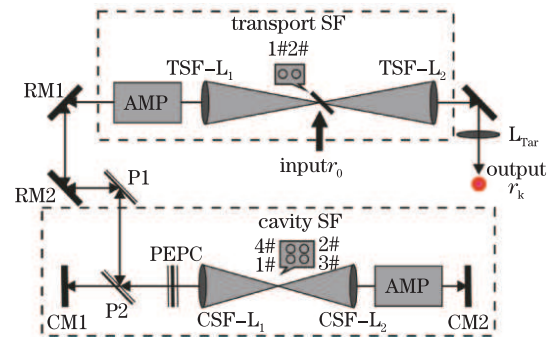


Fig. 3. Structure of the four-pass amplifier system.

Table 1. Optical Parameters and Sensitivities of Lenses in the Pre-amplifier

Imaging Unit	Lens $L_i$	Focal Length $f_i(\text{mm})$	Sensitivity $q_i$	Sensitivity $w_i$
IU <sub>1</sub>	L <sub>1</sub>	1 500	0.3442	1.6520
	L <sub>2</sub>	1 500	0.3442	1.6520
IU <sub>2</sub>	L <sub>3</sub>	1 300	0.3917	1.9062
	L <sub>4</sub>	2 080	0.3917	1.1913
IU <sub>3</sub>	L <sub>5</sub>	1 920	0.4302	1.2906
	L <sub>6</sub>	2 880	0.4302	0.8604
IU <sub>4</sub>	L <sub>7</sub>	1 200	1.0325	2.0650
	L <sub>8</sub>	2 400	1.0325	1.0325
	L <sub>9</sub> (L <sub>Tar</sub> )	2 478	1.0000	1.0000

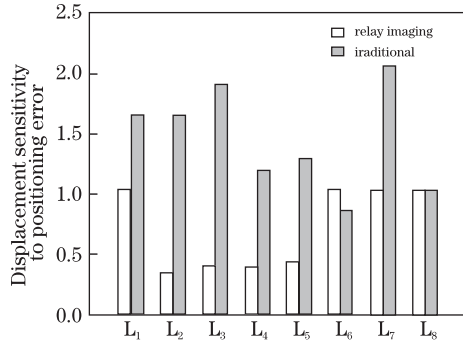


Fig. 4. Sensitivities of lenses in the pre-amplifier.

A similar comparison has been made for the four-pass amplifier system. In this instance, the beam passes through the optics more than once. The structure of the four-pass amplifier system is shown in Fig. 3, which includes three parts: the transport SF (TSF), the cavity SF (CSF), and the coupling part<sup>[3,8]</sup>. The TSF mainly includes two lenses (TSF-L<sub>1</sub> and TSF-L<sub>2</sub>), a pinhole plate (#1 and #2), and slab amplifiers (AMP). The CSF

mainly comprises two lenses (CSF-L<sub>1</sub> and CSF-L<sub>2</sub>), two cavity mirrors (CM1 and CM2), a pinhole plate (#1, #2, #3, and #4), AMP, and a plasma electrode Pockels cell (PEPC). The coupling part comprises two polarizers (P1 and P2) and two reflecti mirrors (RM1 and RM2).

A polarized beam is injected through pinhole #1 in the TSF with input beam pointing error  $\Delta r_0$ . After passing through both TSF-L<sub>1</sub> and the amplifier, the beam is reflected into the CSF by mirrors RM1 and RM2 and by polarizers P1 and P2, respectively. Then, the beam passes four times through CSF-L<sub>1</sub>, the pinholes, CSF-L<sub>2</sub> and the amplifier, through the polarization change action of the PEPC. Afterwards, it is deflected out of the CSF by P2, and then traverses CSF-L<sub>1</sub>, pinhole #2, and CSF-L<sub>2</sub> in the TSF. Finally, the beam passes through the target lens L<sub>Tar</sub> and focuses on the target.

Regardless of the reflection element, such as RM and P, this four-pass amplifier system can be considered as a relay imaging system (Fig. 5).

The respective optical parameters and sensitivities of every lens in the four-pass amplifier system obtained using Eqs. (11) and (13) are listed in Table 2. Considering these lenses are traversed by the beam twice or four times, they are repeated in Fig. 5 with different sensitivities  $q_{k,1}$  from Eq. (11). The total value of lens sensitivity  $Q_i$  is the sum of  $q_{k,1}$  for the same lens, and is given as

$$\begin{cases} Q_{\text{TSF-L}_1} = q_{1,1} + q_{5,2} = 2f_{\text{Tar}}/f_{\text{TSF-L}_2} \\ Q_{\text{CSF-L}_1} = q_{1,2} + q_{3,1} + q_{3,2} + q_{5,1} = 4 \frac{f_{\text{Tar}} f_{\text{TSF-L}_1}}{f_{\text{TSF-L}_2} f_{\text{CSF-L}_1}} \\ Q_{\text{CSF-L}_2} = q_{2,1} + q_{2,2} + q_{4,1} + q_{4,2} = 4 \frac{f_{\text{Tar}} f_{\text{TSF-L}_1}}{f_{\text{TSF-L}_2} f_{\text{CSF-L}_1}} \\ Q_{\text{TSF-L}_2} = q_{6,1} = f_{\text{Tar}}/f_{\text{TSF-L}_2} \end{cases} \quad (18)$$

Given that the lenses have approximate (equal) focal lengths in CSF (TSF), as shown in Table 2, these two methods give much the same results as the sensitivities shown in Fig. 6. To further analyze the impact of focal length change on sensitivities, the value of  $f_1$  is changed to 12 000 mm. The resulting sensitivities of the lenses in the new system are shown in Fig. 7.

Table 2. Optical Parameters and Sensitivities of Lenses in the Four-pass Amplifier

Imaging Unit	Lens $L_{k,1}$	Focal Length $f_{k,1}(\text{mm})$	Sensitivity $q_{k,1}$	Lens $i$	Sensitivity $Q_i$	Sensitivity $w_i$
IU <sub>1</sub>	L <sub>1,1</sub>	16 000	0.1187			
	L <sub>1,2</sub>	11 883	0.1599	TSF-L <sub>1</sub>	0.2375	0.2375
IU <sub>2</sub>	L <sub>2,1</sub>	11 117	0.1599	(L <sub>1,1</sub> ; L <sub>5,2</sub> )		
	L <sub>2,2</sub>	11 117	0.1599	CSF-L <sub>1</sub>		
IU <sub>3</sub>	L <sub>3,1</sub>	11 883	0.1599	(L <sub>1,2</sub> ; L <sub>3,1</sub> ;	0.6396	0.6396
	L <sub>3,2</sub>	11 883	0.1599	L <sub>3,2</sub> ; L <sub>5,1</sub> )		
IU <sub>4</sub>	L <sub>4,1</sub>	11 117	0.1599	CSF-L <sub>2</sub>		
	L <sub>4,2</sub>	11 117	0.1599	(L <sub>2,1</sub> ; L <sub>2,2</sub> ;	0.6396	0.6836
IU <sub>5</sub>	L <sub>5,1</sub>	11 883	0.1599	L <sub>4,1</sub> ; L <sub>4,2</sub> )		
	L <sub>5,2</sub>	16 000	0.1188			
IU <sub>6</sub>	L <sub>6,1</sub>	16 000	0.1188	TSF-L <sub>2</sub>	0.1188	0.1188
	L <sub>6,2</sub>	1 900	1.0000	(L <sub>6,1</sub> )		

To analyze the phenomena shown in Figs. 4, 6, and 7, Eq. (17) is re-discussed below.

- In Fig. 4, the different results between two methods are due to the magnifications of SFs, specifically,  $M_k$  is not equal to 1 in Eq. (17). In contrast, the same result appears in Fig. 6 for the approximate (equal) focal lengths of their SFs.

- Beam expansion is one of the main functions of SFs; thus, the product of  $M_k$  in the ICF system is generally bigger than 1. As a result, traditional sensitivity values become higher than relay imaging values, as shown in Fig. 4.

- In the traditional method, the sensitivity of the lens is only affected by its own focal length, which is why  $L_3$  is much more sensitive than  $L_8$  in Fig. 4.

- In the relay imaging method, the sensitivity of the lens is affected by the other lenses located next to it along the beam path. We intentionally changed the focal length of TSF- $L_1$ , and as a result, the sensitivities of the front lenses changed (e.g., CSF- $L_1$  and CSF- $L_2$ ), but those behind the lens did not (TSF- $L_2$ ) (Fig. 7).

In conclusion, the model of a beam propagating in a high power laser system is built based on relay imaging. The displacement sensitivity of the lens to the beam positioning error has been obtained using this model, which is then compared with the traditional method. Two real systems, the pre-amplifier and the four-pass amplifier, have been depicted to further discuss the differences between these two methods. From the above discussion, the range of application can be summarized as

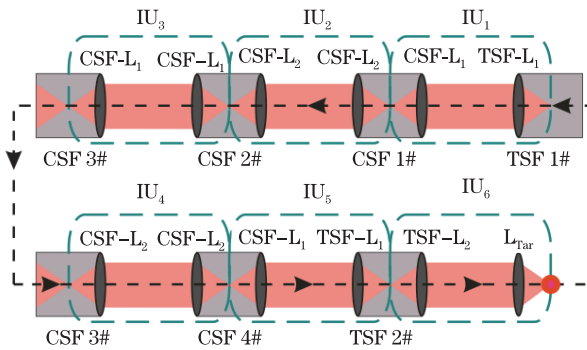


Fig. 5. Structural sketch of the four-pass amplifier system.

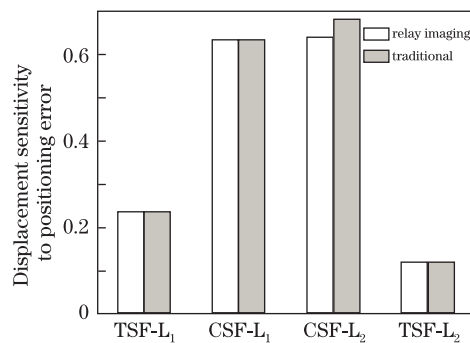


Fig. 6. Sensitivities of lenses in the four-pass amplifier ( $f_1 = 16000$  mm).

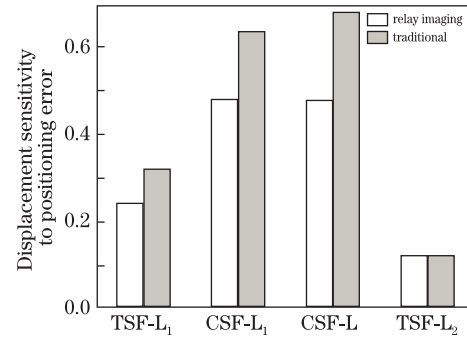


Fig. 7. Sensitivities of lenses in the four-pass amplifier ( $f_1 = 12000$  mm).

- If the whole system is combined with sequential  $4f$ -SFs, these two methods are congruent. The traditional method is recommended in this case for its simple expression.

- Except the above case, the focal length of the lens should not be considered as the only factor of its sensitivity ( $f_{Tar}$  is constant). Actually, the sensitivity of the lens is also affected by the others that located next to it along the beam path, or it could be that it has nothing to do with its own focal length, as exemplified by TSF- $L_1$  and CSF- $L_2$  in Eq. (18). In this instance, the method based on relay imaging is recommended.

- By adjusting the magnifications of IU,  $m_k$  (or the magnifications of SF,  $M_k$ ), the sensitivities of the lenses can be more harmonized in a high power laser system, with the improvement of whole beam stability.

This work was supported by the Chinese and Israeli Cooperating Research on High Power Laser Technology under Grant No. 2010DFB70490.

## References

1. J. T. Hunt, J. A. Glaze, W. W. Simmons, and P. A. Renard, *Appl. Opt.* **17**, 2053 (1978).
2. Y. Zhang, X. Li, P. Sun, and J. Zhu, *Chin. Opt. Lett.* **8**, 210 (2010).
3. Y. Gao, B. Zhu, D. Liu, X. Liu, and Z. Lin, *Appl. Opt.* **48**, 1591 (2009).
4. F. Liu, J. Zhu, J. Xu, Q. Shan, K. Xiao, and X. Zhang, *Chin. Opt. Lett.* **10**, 041402 (2012).
5. J. Xu, F. Liu, P. Yang, and J. Zhu, *Chinese J. Lasers* (in Chinese) **38**, 1002001 (2011).
6. D. J. Trummer, R. J. Foley, and G. S. Shaw, in *Proceedings of the Third International Conference on Solid State Lasers for Application to Inertial Confinement Fusion* 363 (1999).
7. J. Zhang, H. Zhou, Y. Zhou, B. Feng, S. Wang, D. Lin, and F. Jing, *High Power Laser and Particle Beams* (in Chinese) **20**, 1129 (2008).
8. C. A. Haynam, P. J. Wegner, J. M. Auerbach, M. W. Bowers, S. N. Dixit, G. V. Erbert, G. M. Heestand, M. A. Hennesian, M. R. Hermann, K. S. Jancaitis, K. R. Manes, C. D. Marshall, N. C. Mehta, J. Menapace, E. Moses, J. R. Murray, M. C. Nostrand, C. D. Orth, R. Patterson, R. A. Sacks, M. J. Shaw, M. Spaeth, S. B. Sutton, W. H. Williams, C. C. Widmayer, R. K. White, S. T. Yang, and B. M. Van Wonterghem, *Appl. Opt.* **46**, 3276 (2007).